Assessment of the operation of a pre-chamber marine engine fuelled by ammonia-hydrogen mixtures at full and partial load

G. D'Antuono, D. Lanni*, E. Galloni, G. Fontana
Department of Civil and Mechanical Engineering, University of Cassino and Southern Lazio, Cassino, Italy

*E-mail: davide.lanni@unicas.it

Abstract. Carbon-free fuels can play a crucial role in the decarbonization of the maritime sector. This research examines the operation of a pre-chamber marine engine fuelled with ammonia-hydrogen mixtures. The study is carried out by means of a previously validated three-dimensional computational fluid dynamics model. Both full and partial load conditions have been assessed. At full load with 15% hydrogen in the fuel mixture, a spark angle of 716° is necessary to avoid knocking. The engine can achieve an $IMEP_H$ of 29 bar, approximately 43% efficiency, and a gross power output of 1.1 MW per cylinder. In these conditions, unburned ammonia and NO_2 emissions are relatively low, N_2O emissions are zero, while NO remains the main pollutant. At partial load conditions, a fuel mixture that contains 15% hydrogen by volume does not enable acceptable engine operation, whereas a 30% hydrogen content results in suitable operating conditions.

1. Introduction

Currently, due to the significant impact that traditional fuels are having on the climate, and in order to comply with existing regulations, the study of carbon-free fuels has become essential. Following this direction, ammonia [1-2] can be a viable solution to substitute conventional fuels like gasoline or diesel. Unfortunately, ammonia shows a very low laminar flame speed (87% less than gasoline) [2]; therefore, it is very useful to consider also its blends with other fuels. By maintaining a completely carbon-free mixture, hydrogen emerges as the optimal solution for enhancing the combustion properties of ammonia [3-6]. To enhance the analyses of different ammonia-hydrogen blends, recent investigations were focused on correlations that assist in estimating both the laminar flame speed [7-8] and the ignition delay [9].

Lhuillier et al. [10] conducted a study on the combustion characteristics of a spark ignition engine fuelled by ammonia-hydrogen mixtures, revealing that hydrogen enhances engine performance. However, they also found that when the engine load diminishes or the engine speed surpasses 2000 rpm, the stability of combustion continues to be inadequate. Additionally, the levels of unburned ammonia are significantly elevated in all scenarios. Pyrc et al. [11] conducted an experimental study on a spark ignition (SI) engine that featured a variable pressure ratio, which they modified to operate as a dual-fuel engine utilizing ammonia and hydrogen. They examined two distinct pressure ratios (8 and 10) and varied the proportion of energy supplied by hydrogen from 0 to 70%. The findings indicate that when 12% of the energy is derived from hydrogen, the instability associated with the ignition process is eliminated. Specifically, at a compression ratio of 8, the authors noted that the ignition delay is reduced by half, whereas at a compression ratio of 10, it is reduced by nearly two-thirds; correspondingly, the specific energy consumption diminishes as the compression ratio is increased.

These results clearly show the potential of ammonia-hydrogen blends as a fuel blend; furthermore, the hydrogen required for the combustion process can be obtained directly from ammonia through a cracking process. In [12], Zhang et al. conducted a numerical analysis investigating the combustion characteristics of a spark-ignition engine fuelled by ammonia-hydrogen mixtures, where hydrogen was generated via the reforming of exhaust fuel. Their findings indicated that incorporating hydrogen, at concentrations up to 10% by volume, resulted in elevated cylinder pressure and a decrease in the combustion duration. Frigo et al [13-14] proposed a cracking system for an engine used as a range extender for electric vehicles, which is powered by ammonia and hydrogen derived from ammonia. The authors demonstrated that the quantity of hydrogen required to enhance combustion velocity is primarily influenced by the load rather than the engine speed. Specifically, they noted a hydrogen percentage of 6% (by volume) at full load and 10% at partial load. Klawitter et al. [15] explored the combustion properties of an ammonia engine while considering partially cracked ammonia. They analysed ammonia cracking ratios of 0%, 7.5%, and 10%, in conjunction with equivalence ratios that varied from 0.7 to 1.2, while adjusting for engine speed and turbulence. Their results demonstrated that partial ammonia cracking improved combustion efficiency. In conclusion, they observed flame speed values that were similar to those of methane when the ammonia cracking ratio reached 10%.

All the literature results presented clearly show that ammonia hydrogen blends can be used instead of conventional fuels, however, especially for heavy duty engine, further enhancement of the combustion process can be achieved through structural modifications of the engine, such as the use of multiple spark plugs [16] or the utilization of a suitably sized pre-chamber. Udden et al. [17] conducted an experimental investigation on the combustion and flame characteristics within a spark-ignition engine, emphasizing a method that utilizes multiple sparks. The findings presented in their study indicate that a single spark plug positioned centrally in the combustion chamber resulted in a reduced heat release rate and a lower pressure peak. Conversely, the implementation of multiple spark plugs led to an increased heat release rate, heightened cylinder pressure, and a shorter duration of combustion. The authors also observed a decrease in cyclic variation attributed to the higher pressure within the combustion chamber. Furthermore, the flame analysis demonstrated that employing multiple spark plugs enabled quicker flame propagation in comparison to a single spark configuration. Huang et al. [18] examined the impact of multiple spark plugs on the combustion dynamics of a compression ignition engine that was modified to work as a spark-ignition engine using ammonia. Their results demonstrated that the use of multiple spark plugs resulted in an increased burn rate and power output, a reduced combustion duration, lower unburned ammonia emissions, and enhanced fuel efficiency. Importantly, they observed that the incorporation of multiple sparks did not lead to an increase in NOx emissions.

The research findings clearly illustrate that ammonia achieves better combustion at high loads and low speeds. These conditions are inherent to marine engines; thus, the use of ammonia and hydrogen as fuels for the maritime sector is currently being investigated. Moreover, more than 80% of international goods trade is carried out by sea, and this ratio is notably higher in the majority of developing countries. Globally, this represents about 2% of global CO_2 emissions. This emphasizes the critical need for the maritime industry to adopt carbon-free fuels to reduce its environmental impact. Recently, Huo et al. [19] investigated the impact of the hydrogen energy

Journal of Physics: Conference Series **3143** (2025) 012098 doi:10.1088/1742-6596/3143/1/012098

fraction, equivalence ratio, and ignition timing on the combustion and emission characteristics of an ammonia-hydrogen mixture, specifically under lean combustion conditions in a pre-chamber marine engine. The authors observed that an increase in the hydrogen fraction and equivalence ratio within the main chamber leads to a significant rise in combustion pressure, temperature, and heat release rate (HRR). This heightened reactivity results in a decrease in combustion duration, which may lead to end gas auto-ignition and knocking due to the reduced auto-ignition energy of the mixture. Given that detonation is a phenomenon to be avoided, such configurations may be integrated with strategies designed to mitigate the risk of knock [20-21]. In [22], Indlekofer et al. utilize Large Eddy Simulation (LES) methodologies to investigate the ignition and combustion dynamics of an ammonia primary charge that is ignited by a hydrogen-driven prechamber. The authors note that the timing and angle of injection between the liquid sprays and the hydrogen jet flames that emerge from the prechamber have a significant impact on the ignition and combustion processes. Furthermore, the non-premixed configuration of the ammonia main charge considerably reduces pollutant emissions and broadens the operational range to leaner global equivalence ratios, in contrast to the premixed ammonia main charge configuration.

Given the restricted findings available on this topic, this paper proposes a CFD analysis aimed at investigating the operation of a passive pre-chamber marine engine fuelled by ammonia-hydrogen fuel mixtures. Performances at maximum brake torque at knock limit are presented for both full load and partial load operation, adjusting the hydrogen required to guarantee a proper combustion at partial load. The engine speed for all the investigated points was fixed and equal to 500 rpm, which is a typical cruise velocity for this kind of engine.

2. Methodology

The engine considered for the analyses and presented in Table 1 has been designed taking inspiration from the renowned WR6L46 engine produced by Wärtsilä. This marine engine, originally developed to work as a diesel engine, operates on a four-stroke cycle and has a medium speed range of 300 to 1000 rpm. It features a flat-head cylinder design with four valves for each cylinder. The geometrical compression ratio is established at 12.5, as in [23], where a similar engine was analyzed for dual fuel functionality. Additionally, the engine is equipped with a piston bowl designed to accommodate fuel jets originating from the pre-chamber. The pre-chamber has been created in accordance with the design specified in [24] for a similar engine. It is situated on the cylinder head, aligned with the cylinder axis, and features six nozzles that are angled at 20 degrees in relation to the cylinder axis. The volume of this pre-chamber represents 0.8% of the overall combustion chamber volume. The nozzle diameter has been chosen equal to 5 mm. Figure 1 presents the computational grid used, characterized by a total of 134884 elements at TDC and 478720 elements at EVO, with the dimension of an element equal to 4.5 mm. It has been chosen according to the grid sensitivity analysis reported in section 2.2.

Table 1. Main Engine Characteristics

Bore [mm]	460
Stroke [mm]	580
Connecting rod length [mm]	650
Compression ratio [-]	12.5
Displacement per cylinder [l]	96.4
Prechamber volume [cm^3]	67.1
Inlet valve closing angle [°bTDC]	120
Exhaust valve closing angle [°aTDC]	128

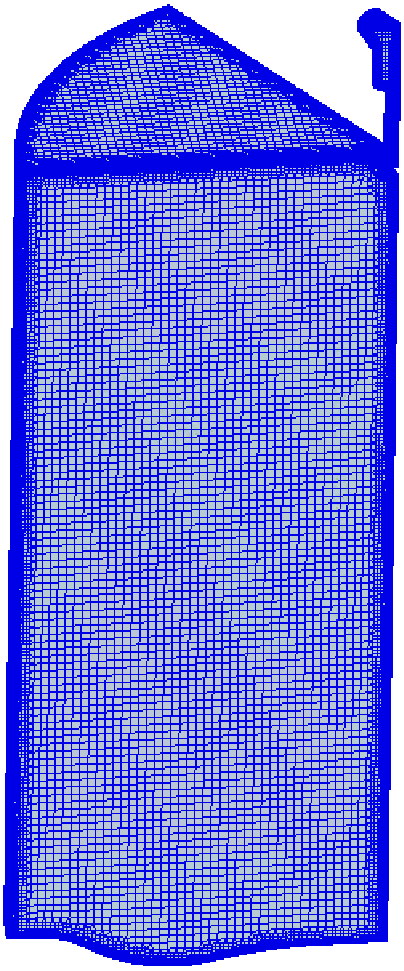

Figure 1. Computational grid.

2.1 3D CFD Model

Analyses have been conducted utilizing a 3D numerical approach, in which simulations start at the intake valve closing (IVC) and end at the exhaust valve opening (EVO). Calculations have been carried out on a dedicated workstation equipped with an Intel® Xeon® w9-3495X processor. A total of 25 physical cores were employed for the computations, with 128 GB of system memory available. The simulation of a single engine operating point required about 50 hours.

Journal of Physics: Conference Series **3143** (2025) 012098 doi:10.1088/1742-6596/3143/1/012098

The proposed model was already developed and validated on a light-duty engine [25]. Briefly, the balance equations that govern the unsteady, turbulent, and chemically reacting flow within the chamber are resolved utilizing the AVL Fire code [26] through a RANS (Reynolds-Averaged Navier-Stokes) approach [27-28]. The k-z-f methodology has been integrated with the Reynolds-averaged transport equations to effectively model the turbulent effects [29]. The k-z-f turbulence model is a RANS closure approach developed to accurately capture near-wall turbulence without the use of empirical damping functions. It employs the velocity scale ratio (z) and an elliptic relaxation function (f) to enhance predictions in separated flows, low-Reynolds-number regions, and adverse-pressure-gradient conditions [29]. This approach has been selected due to its proficiency in accurately capturing flow characteristics near the wall, in line with a hybrid wall treatment. Heat transfer across the walls is represented through a conventional wall function. The oxidation process of ammonia-hydrogen fuel mixtures has been simulated by integrating the chemical kinetics mechanism proposed by Stagni et al. [30] (summarized in Table 2) into the three-dimensional model. This mechanism has been chosen because it provides good accuracy in reproducing experimental results [9, 25]. Furthermore, in its latest release, it also considers the decomposition of ammonia, the H-abstractions, and the dissociation of the HNO intermediate. Furthermore, it also considers the formation of NO due to both the dissociation of ammonia and the oxidation of nitrogen contained in the air.

Ignition has been successfully replicated by introducing a specific amount of energy into a sphere with a diameter of 3 mm. The placement of this sphere corresponds with the location of the spark-plug electrodes, and the energy release is adjusted in accordance with literature data. The energy release by the sphere has been chosen starting from the one used to validate the experimental data in [25] and adjusted considering the different engine size.

Table 2. Chemical kinetic mechanism details [30]

Number of species	31
Number of reactions	203
Main Species	NH_3, H_2, N_2, O_2, OH, NO, N_2O, NO_2
Overall equivalence ratio [-]	0.8-1.4

Simulations have been initialized considering the wall temperature characteristics for the WR46 engine from the literature. The charge was initially considered as stationary, with the initial turbulent intensity defined as 10% of the average piston speed, and the initial integral length scale assumed to be 10% of the diameter of the domain under consideration, as usual for this kind of simulation. In both the pre-chamber and the main chamber, the temperature, pressure, and charge composition at IVC have been determined through preliminary one-dimensional calculations performed in the GT-Suite environment [31].

To evaluate the knock occurrence in the investigated engine, the spark advance has been varied to obtain the minimum knock onset, calculated as expressed in equation 1, when the burned fuel fraction reached the 90%:

$$KO = \int_0^t \frac{1}{\tau_{id}(P_{EG}, T_{EG}, \Phi_{EG})} dt \tag{1}$$

In particular, KO stands for Knock-Onset, while τ_{id} is the ignition delay calculated in the Cantera environment [32], as a function of the pressure, temperature, and equivalence ratio of the end gas mixture in the combustion chamber. The Cantera environment is an open-source software suite for the modeling of chemical kinetics, thermodynamics, and transport phenomena. It is

Journal of Physics: Conference Series **3143** (2025) 012098 doi:10.1088/1742-6596/3143/1/012098

extensively employed for the simulation of combustion systems, reactors, flames, and electrochemical processes [32]. When the KO becomes equal to 1, there is a knock possibility.

2.2 Grid sensitivity

A preliminary analysis aimed to define the best grid dimension has been done by developing 3 different unstructured grids, considering hexahedral elements with a fixed dimension that varies from 4 mm to 5 mm. Considering an ammonia-hydrogen fuel mixture, characterized by an equivalence ratio equal to 0.8 and a hydrogen amount of 15% by volume, the three different computation grids have been tested. The results, presented in Figure 2 and Table 3, clearly show that the intermediate and finest grids exhibit a combustion development that is both very similar and more rapid than that observed in the coarsest grid. When examining the pressure peak, the coarsest grid displays a difference of approximately 5% in comparison to the intermediate grid, whereas the latter shows a mere 1% difference relative to the finest grid. This same pattern is illustrated in Table 3 regarding combustion duration; specifically, the transition from the coarsest grid to the intermediate grid results in a variation of about 6% in CA 0-10, while the comparison between the finest and intermediate grids reveals only a 2% difference.

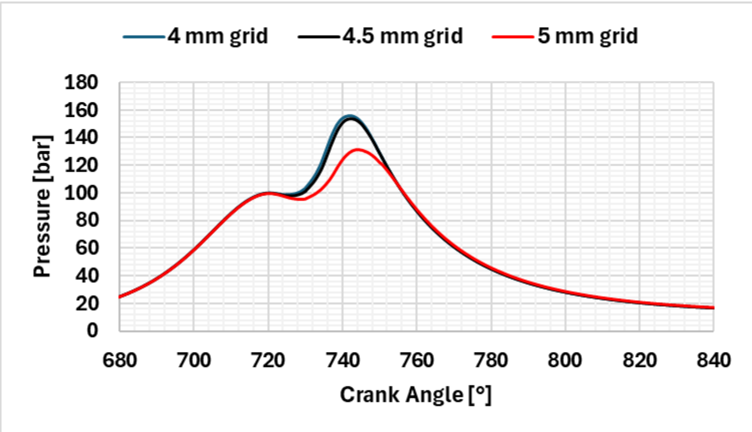

Figure 2. In-cylinder pressure for different cell sizes.

Table 3. Combustion durations for the different meshes investigated. CA0-10 is the 0-10% mass fraction fuel burn duration, CA50 is the crank angle after TDC at 50% mass burning fraction, and CA10-90 is the 10-90% mass fraction fuel burn duration.

Cell size [mm]	4	4.5	5
CA0-10 [°]	18.2	18.6	19.8
CA50 [°aTDC]	13.6	13.6	17.8
CA10-90 [°]	17	17.4	20.2

Considering the presented results, the intermediate grid has been used for all the simulations presented in the following section.

3. Results

3.1 Full load conditions

First, full-load simulations were conducted considering a hydrogen enrichment equal to 15% by volume, adhering to the conditions outlined in Table 4, with the objective of determining the optimal spark angle and also performing a preliminary analysis of knock. In particular, the spark advance has been chosen considering the crank angle that provides the best $IMEP_H$ (gross indicated mean effective pressure) and efficiency without a knock onset, evaluated using the relation presented in equation 1.

Table 4. First set of simulation initial conditions

Hydrogen amount by volume [%]	15
Engine speed [rpm]	500
Equivalence ratio [-]	0.8
Intake pressure [bar]	3.45
Exhaust pressure [bar]	3
Intake temperature [K]	323
Exhaust temperature [K]	323
Spark Angle [°]	708-716
Burned mass fraction at knock onset [-]	0.9

Figures 3 and 4 present the in-cylinder pressure and temperature curves. From Figure 3, it is clear that the spark angle closest to the TDC is unable to provide a knock occurrence. The more the spark angle is advanced, the more the slope of the curves increases, leading to a Knock Onset close to 1. Also, the temperature curves show the same trends, with the more advanced spark angle corresponding to the higher curve slope. Table 5 presents the results of the knock occurrence analysis.

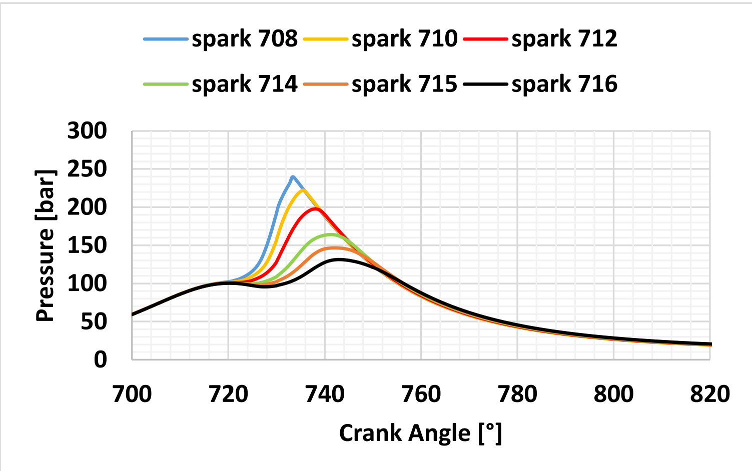

Figure 3. In-cylinder pressure for 15% of hydrogen by volume, varying the spark advance.

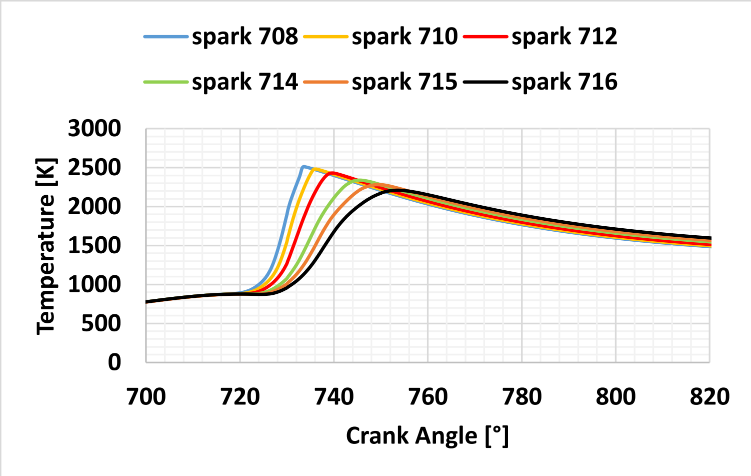

Figure 4. In-cylinder temperature for 15% of hydrogen by volume, varying the spark advance.

Table 5. Knock occurrence analyses for 15% of hydrogen by volume

Spark Angle [°]	708	712	713	714	715	716
$IMEP_H$ [bar]	32.3	32.0	31.6	30.7	30.0	29.2
Power [kW]	1298.0	1287.0	1268.4	1232.5	1205.7	1171.6
Efficiency [%]	48	47.6	46.9	45.6	44.6	43.4
Knock Onset Angle [°]	730.7	732.5	734.9	739.9	745.5	-
Mass burned at knock Onset [%]	70.4	71.5	71.7	77.7	87	-

From Table 5, it is worth noting that with 15% of hydrogen by volume, almost all the investigated points present a knock onset equal to or greater than one; therefore, only a spark angle equal to 716° is feasible. It is also worth noting that the no-knock conditions found for this blend present the lower values for the $IMEP_H$, the power, and the efficiency related to the combustion process. The choice to consider acceptable only the spark angles corresponding to a knock onset less than one is conservative and has been made because it was not possible to further investigate the knock using this methodology. Future studies will be conducted to explore the phenomenon of knock in greater depth and to verify whether all the excluded points are indeed not tolerable by the engine.

Figures 5 and 6 show the in-cylinder pressure, in-cylinder temperature, and rate of heat release curves considering full load conditions. Both pressure and temperature peaks remain in an acceptable range, ensuring the structural integrity of the engine. Furthermore, the rate of heat release curves presents a peak of about 34 kJ/deg with a small spike at around 750 crank angle indicating that also for this spark advance a portion of the end gas could potentially auto ignite, but this does not present a risk of detonation that might compromise the engine structural integrity. This is also confirmed by the result obtained using equation 1, which provides a value of the integral equal to 0.94, close to the value of 1, but undoubtedly secure. Considering the performance, the engine in these conditions is able to guarantee an $IMEP_H$ equal to 29 bar, with an efficiency of about 43% and a gross power equal to 1.1 MW per cylinder. These values did not consider the pumping loss; therefore, there is surely a slight overestimation, but also considering the pumping loss, these values remain comparable to the maximum ones of a typical diesel engine, suggesting that ammonia-hydrogen blends can be used in substitution of conventional fossil fuels. In the end, Table 6 presents the combustion durations for this fuel blend. The values obtained, even if they are higher than those typically found in a conventional engine, still remain in an acceptable range.

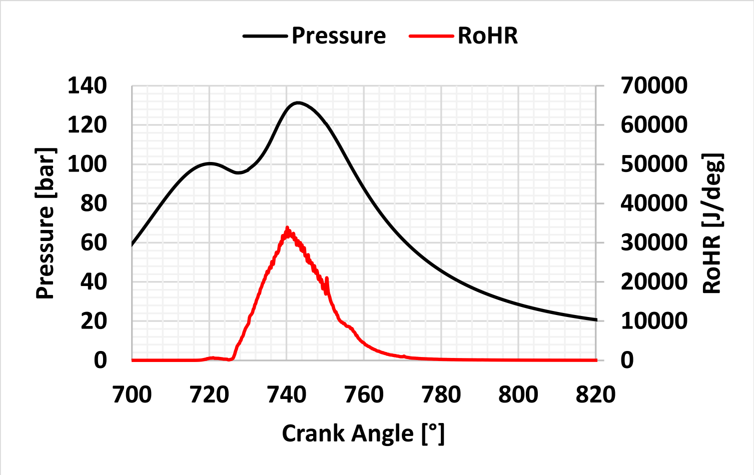

Figure 5. In-cylinder pressure and rate of heat release. Full load.

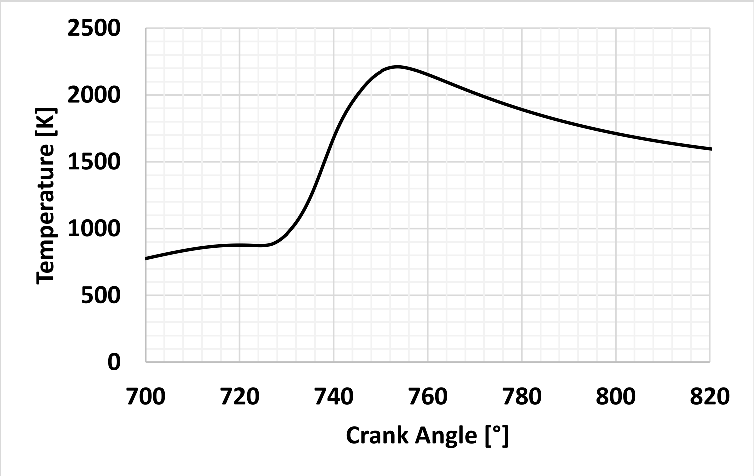

Figure 6. In-cylinder temperature. Full load.

Table 6. Combustion durations. Full load. CA0-10 is the 0-10% mass fraction fuel burn duration, CA50 is the crank angle after TDC at 50% mass burning fraction, and CA10-90 is the 10-90% mass fraction fuel burn duration.

CA0-10 [°]	15.8
CA50 [°aTDC]	20.2
CA10-90 [°]	34.2

For an ammonia-hydrogen engine, it is also crucial to consider the emissions related to the combustion process. In particular, both the NOx and unburned ammonia were analyzed, since unburned ammonia is a very dangerous substance for humans if inhaled. Table 7 summarizes the amount of each of these substances. It is worth noting that unburned ammonia does not present high values, but it is still mandatory to couple the engine with a selective catalytic reactor. The NOx presented at EVO considers both the thermal mechanism and the fuel mechanism, since ammonia presents nitrogen in its molecule. The NO remains the main issue that must be addressed, while NO_2 is relatively contained at EVO since it is a nitrogen oxide formed during a secondary process that occurs when atmospheric NO combines with oxygen. In any case, even the NO can be effectively managed using the conventional treatment systems for this pollutant that are already available on board ships for conventional fuels. N_2O is equal to 0, and this can be explained considering that it is primarily produced in the regions with low ammonia concentrations at temperatures under 1400 K [33], a condition that does not occur at the considered operating point, as also shown in Figure 6, in which the temperature is always greater than 1500K.

Table 7. Emissions

NH_3 unburned [ppm]	54
NO [ppm]	5205
N_2O [ppm]	0
NO_2 [ppm]	75

3.2 Partial load conditions

To assess the feasibility of employing this mixture in the analysed engine, a partial load condition has also been tested. In particular, an intake pressure equal to 1 bar has been considered, keeping the same spark advance.

Unfortunately, as shown in Figures 7 and 8, this ammonia-hydrogen fuel mixture is not able to guarantee proper engine operation. In particular, both the in-cylinder pressure, in-cylinder temperature, and rate of heat release curves are far from an acceptable engine condition.

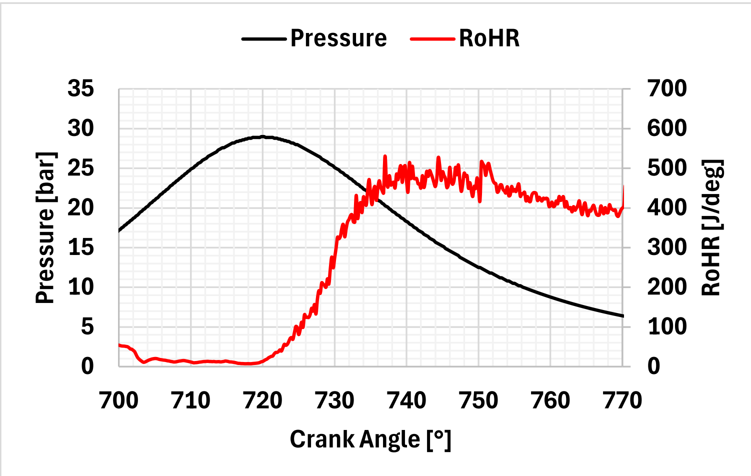

Figure 7. In-cylinder pressure and rate of heat release. Partial load condition. 15% of hydrogen in the fuel blend.

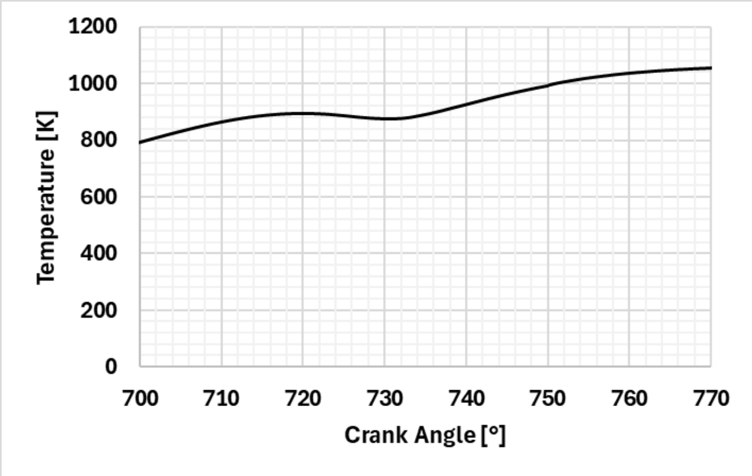

Figure 8. In-cylinder temperature. Partial load condition. 15% of hydrogen in the fuel blend.

The results presented above clearly show that for no boost conditions, 15% of hydrogen by volume is not usable, and also, a variation in the spark timing cannot lead to a proper combustion process. However, this may not be a critical aspect since hydrogen, as already discussed, can be produced directly from ammonia cracking, and considering the size of the ships on which this engine is typically installed, there are no significant issues related to the dimensions of the cracking reactor. Therefore, an ammonia-hydrogen fuel blend characterized by 30% hydrogen by volume has been tested, keeping the same spark advance. Figures 9 and 10 show the in-cylinder pressure, RoHR, and temperature curves. It is worth noting that varying the hydrogen enrichment in the fuel blend allows for the extension of the operational range of the engine. Table 8 summarises the performances and emissions of the engine for the considered conditions. The performance obtained allows the use of the investigated blend also in partial load conditions. Referring to the management of the emissions, especially unburned NO, the coupling of the engine with a specific after-treatment system can reduce their amounts.

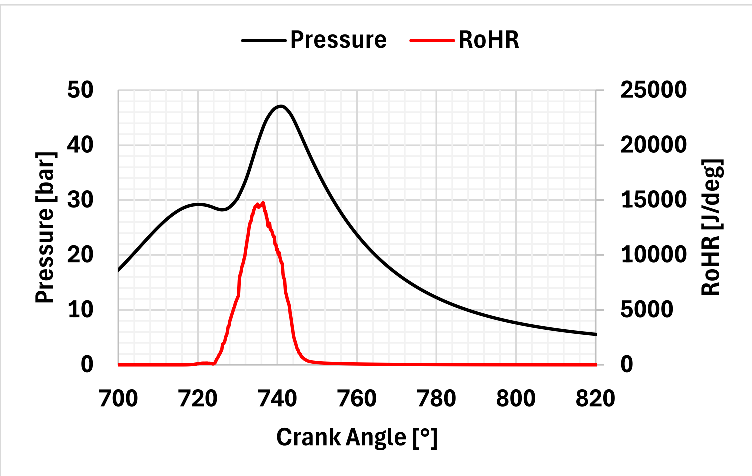

Figure 9. In-cylinder pressure and rate of heat release for 30% of hydrogen in the fuel blend. Partial load condition.

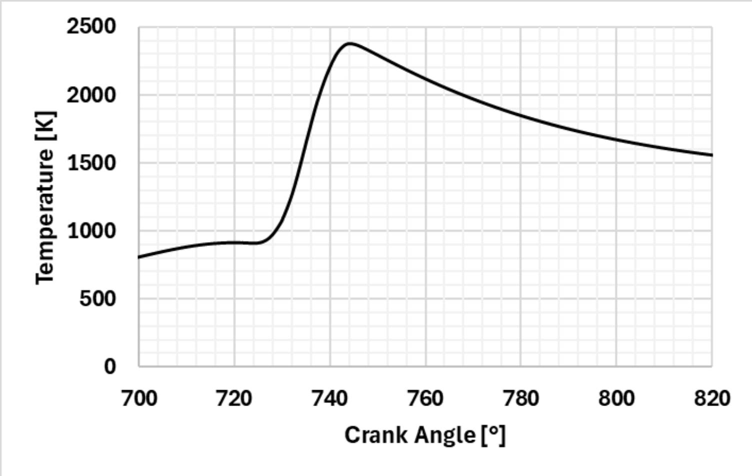

Figure 10. In-cylinder temperature for 30% of hydrogen in the fuel blend. Partial load condition.

Table 8. Performance and emissions at no boost conditions

Spark angle [CAD]	716
$IMEP_H$ [bar]	8.3
Efficiency [%]	29.4
CA 0-10 [CAD]	14
CA 50 [°aTDC]	15.8
CA 10-90 [CAD]	15.2
Unburned NH_3 [ppm]	56
NO [ppm]	6714
N_2O [ppm]	32
NO_2 [ppm]	0

In the end, a variation of the hydrogen amount in the fuel blend allows the use of the engine fuelled mainly by ammonia for the different engine operating conditions.

4. Conclusions

This study presents a numerical analysis focused on examining the operation of a passive pre-chamber marine engine powered by ammonia-hydrogen fuel mixtures. The analysis has been carried out by using a previously validated 3D-CFD model.

The main findings are summarized below:

- At full load, considering 15% of hydrogen by vol. in the fuel blend, only a spark angle equal to 716° is acceptable to avoid knock onset.
- The engine can guarantee an $IMEP_H$ equal to 29 bar, with an efficiency of about 43% and a gross power equal to 1.1 MW per cylinder.
- In the analyzed full load conditions, unburned ammonia and NO_2 emissions are relatively contained, N_2O is equal to 0, while NO is the main issue that must be addressed.
- At partial load, a fuel mixture containing 15% of hydrogen by vol. does not allow an acceptable engine operation, while an amount equal to 30% provides a proper operating condition.

Acknowledgement

This research has been supported by the Italian Government (LYRICA, PRIN project 2022, code 2022M7BHN7).

References

[1] Valera-Medina, A.; Xiao, H.; Owen-Jones, M.; David, W.; Bowen, P. Ammonia for power. Prog. Energy Combust. Sci. 2018, 69, 63–102.
[2] Lanni, D.; Galloni, E.; Fontana, G.; D'Antuono, G. Assessment of the Operation of an SI Engine Fueled with Ammonia. Energies 2022, 15, 8583. https://doi.org/10.3390/en15228583
[3] D'Antuono, G., Lanni, D., Galloni, E., and Fontana, G., "Comparison of the Performance and Operation Limits of an S.I. Engine Fueled with Neat Ammonia and Hydrogen-Ammonia Blends," SAE Technical Paper 2023-24-0042, 2023, doi:10.4271/2023-24-0042.
[4] D'Antuono, G.; Lanni, D.; Galloni, E.; Fontana, G. Numerical Modeling and Simulation of a Spark-Ignition Engine Fueled with Ammonia-Hydrogen Blends. Energies 2023, 16, 2543. https://doi.org/ 10.3390/en16062543
[5] CMørch, S.; Bjerre, A.; Gøttrup, M.; Sorenson, S.C.; Schramm, J. Ammonia/hydrogen mixtures in an SI-engine: Engine performance and analysis of a proposed fuel system. Fuel 2011, 90, 854–864.
[6] Lhuillier, C., Brequigny, P., Contino, F., and Rousselle, C., "Combustion Characteristics of Ammonia in a Modern Spark Ignition Engine," in Proceedings of the Conference on Sustainable Mobility, Catane, Italy, October 14-15, 2019
[7] Goldmann, A.; Dinkelacker, F. Approximation of laminar flame characteristics on premixed ammonia/hydrogen/nitrogen/air mixtures at elevated temperatures and pressures. Fuel 2018, 224, 366–378
[8] Pessina, V., et al. "Laminar flame speed correlations of ammonia/hydrogen mixtures at high pressure and temperature for combustion modeling applications." International Journal of Hydrogen Energy 47.61 10.1016/j.ijhydene.2022.06.007 (2022): 25780-25794.DOI:
[9] D'Antuono, G., Galloni, E., Lanni, D., & Fontana, G. (2024). A Relationship for Estimating the Ignition Delay of Hydrogen Enriched Ammonia-Air Mixtures. Engineered Science, 28, 1074.
[10] Lhuillier C, Brequigny P, Contino F, Rousselle C. Performance and emissions of an ammonia-fueled SI engine with hydrogen enrichment. SAE Technical Paper 2019- 24-0237 2019. https://doi.org/10.4271/2019-24-0137.
[11] Pyrc, M.; Gruca, M.; Tutak, W.; Jamrozik, A. Assessment of the co-combustion process of ammonia with hydrogen in a research VCRpiston engine. Int. J. Hydrogen Energy 2022, 48, 2821–2834.
[12] Zhang, H.; Li, G.; Long, Y.; Zhang, Z.; Wei, W.; Zhou, M.; Belal, B.Y. Numerical study on combustion and emission characteristics of a spark-ignition ammonia engine added with hydrogen-rich gas from exhaust-fuel reforming. Fuel 2023, 332, 125939.
[13] Comotti, M.; Frigo, S. Hydrogen generation system for ammonia–hydrogen fuelled internal combustion engines. Int. J. Hydrogen Energy 2015, 40, 10673–10686.
[14] Frigo, S.; Gentili, R.; Doveri, N. Ammonia plus hydrogen as fuel in a SI engine: Experimental results. SAE Tech. Pap. 2012. [CrossRef]
[15] Klawitter, M., Wüthrich, S., Cartier, P., Albrecht, P., Herrmann, K., Gößnitzer, C., ... & Wimmer, A. (2024). Ammonia as a fuel: Optical investigation of turbulent flame propagation of NH3/Air and NH3/H2/N2/Air flames at engine conditions. Fuel, 375, 132616.
[16] Lanni, D., D'Antuono, G., Galloni, E., Fontana, G., Contino, F., & Brequigny, P. (2025). Improving Ammonia Combustion in Spark-Ignition Engines Coupling Hydrogen Enrichment with Multiple Spark Plugs. Energy & Fuels.
[17] Uddeen, K., Tang, Q., Shi, H., Magnotti, G., & Turner, J. Multiple spark ignition approach to burn ammonia in a spark-ignition engine: An optical study. 2023. SAE Technical Paper.
[18] Huang, Qiao, and Jinlong Liu. "Preliminary assessment of the potential for rapid combustion of pure ammonia in engine cylinders using the multiple spark ignition strategy." International Journal of Hydrogen Energy 55 (2024): 375-385
[19] Huo, J., Zhao, T., Lin, H., Li, J., Zhang, W., Huang, Z., & Han, D. (2024). Study on lean combustion of ammonia-hydrogen mixtures in a pre-chamber engine. Fuel, 361, 130773.
[20] Lanni, D., & Galloni, E. (2022). Direct Water Injection Strategies for Performance Improvement of a Turbocharged Spark-Ignition Engine at High Load Operation (No. 2022-37-0007). SAE Technical Paper.
[21] Tornatore, C., Marchitto, L., & Valentino, G. (2021). Technologies for Knock Mitigation in SI Engines—A Review. Engines and Fuels for Future Transport, 325-349.
[22] Indlekofer, T., Haugen, N. E. L., Førde, O. Ø., & Gruber, A. (2024). Numerical Investigation of Premixed and Non-premixed Ammonia Main Charge Configurations Ignited by a Hydrogen Fired Prechamber.

[23] Drazdauskas, M., & Lebedevas, S. (2024). Optimization of Combustion Cycle Energy Efficiency and Exhaust Gas Emissions of Marine Dual-Fuel Engine by Intensifying Ammonia Injection. Journal of Marine Science and Engineering, 12(2), 309.
[24] Huo, J., Zhao, T., Lin, H., Li, J., Zhang, W., Huang, Z., & Han, D. (2024). Study on lean combustion of ammonia-hydrogen mixtures in a pre-chamber engine. Fuel, 361, 130773
[25] d'Antuono, G., Galloni, E., Lanni, D., Contino, F., Brequigny, P., & Mounaïm-Rousselle, C. (2024). Assessment of combustion development and pollutant emissions of a spark ignition engine fueled by ammonia and ammonia-hydrogen blends. International Journal of Hydrogen Energy, 85, 191 199.
[26] FIRE™ - Thermo-Fluid Dynamics and CFD Simulation Version 2020 R2. (2020) Technical documentation
[27] Girimaji, S. (2006): Partially-Averaged Navier-Stokes Model for turbulence: A Reynolds-Averaged Navier-Stokes to Direct Numerical Simulation bridging method. J. of Applied Mechanics, 73, 413 421
[28] Girimaji, S., Jeong, E. and Srinivasan, R. (2006). Partially-Averaged Navier-Stokes Model for turbulence: Fixed point analysis and comparison with unsteady Partially Averaged Navier-Stokes. J. of Applied Mechanics, 73, 422-429
[29] Popovac, M., & Hanjalic, K. (2007). Compound wall treatment for RANS computation of complex turbulent flows and heat transfer. Flow, turbulence and combustion, 78, 177-202.
[30] Stagni, A., Arunthanayothin, S., Dehue, M., Herbinet, O., Battin-Leclerc, F., Bréquigny, P., Mounaïm-Rousselle, C., & Faravelli, T., Low-and intermediate-temperature ammonia/hydrogen oxidation in a flow reactor: Experiments and a wide-range kinetic modeling. (2023) Chemical Engineering Journal, 471, 144577. DOI: 10.1016/j.cej.2023.144577
[31] GT-Suite Engine Performance Application v2020, Gamma Technologies, LLC
[32] Goodwin, D.G.; Moffat, H.K.; Speth, R.L. Cantera: An Object-Oriented Software Toolkit for Chemical Kinetics, Thermodynamics, and Transport Processes, Version 2.2. 1.; Cantera Developers: Warrenville, IL, USA, 2017 DOI:10.5281/zenodo.6387882
[33] P. Dong, S. Chen, L. Zhang, Z. Zhang, W. Long, Q. Wang, W. Chen. Ammonia diffusion combustion and emission formation characteristics in a single cylinder two stroke engine. Energy 311 (2024) 133432. https://doi.org/10.1016/j.energy.2024.133432